Mineralogy and Petrology (1991) 43: 293–314

Mineralogy and Petrology

© by Springer-Verlag 1991
Printed in Austria

Nephelinite-Carbonatite Liquid Immiscibility at Shombole Volcano, East Africa: Petrographic and Experimental Evidence

B. Kjarsgaard[1,*] and T. Peterson[2]

[1] Department of Geology, The University, Manchester, England
[2] Geological Survey of Canada, Ottawa, Canada

With 9 Figures and 6 Plates

Received April 11, 1990;
accepted January 7, 1991

Summary

We summarize the evidence for silicate-carbonate liquid immiscibility in two nephelinite lavas from Shombole volcano, East Africa, and discuss its significance for carbonatite petrogenesis. The nephelinite lavas contain spherical to irregular globules ≤ 0.5 cm containing low-Sr calcite, Sr–Ca and K–Ba zeolites, fluorite, aegirine, strontianite, and fluorapatite. The globules are interpreted to be magmatic in origin, and represent quenched immiscible carbonate liquid. Most phases in the globules form an interlocking mosaic of euhedral crystals, however, rare blebby intergrowths of calcite and strontianite indicate eutectic crystallization from a melt. The phase assemblages and respective compositions of minerals in the globules and silicate groundmass are nearly identical, indicating that the samples were quenched when two liquids were in near-equilibrium. Experiments with the samples at 200–500 MPa and 975–925 °C have reproduced the natural assemblages (phenocrysts +2 liquids) exactly and the compositions of experimentally generated solid phases closely match the original phenocrysts. The natural and experimentally produced carbonatites are both sövitic (calcite carbonatite) in composition.

The two-liquid experimental data from Shombole are compared with the 300 MPa experimental data of *Freestone* and *Hamilton* (1980) and *Hamilton* et al. (1989), who utilized strongly peralkaline bulk compositions typical of the lavas erupted at Oldoinyo Lengai. Both data sets are nearly coplanar in the tetrahedron Si–(Ca + Mg + Fe^{2+})–(Al + Fe^{3+})–(Na + K) (SCAN), but the tielines have different orientations and the Oldoinyo Lengai bulk compositions generate alkali-rich carbonatitic liquids, rather than sövitic liquids. At both volcanic centers, only one type of extrusive carbonatite is known, and crystal fractionation schemes to generate one carbonatite from another are

* Currently at Geological Survey of Canada, 601 Booth Street Ottawa, Canada K1A OE8.

not supported by the data. Experiments illustrate that the full range of Ca–Mg–(Na + K) carbonatites can be generated by liquid immiscibility from nephelinitic magmas of different compositions.

Zusammenfassung

Nephelinit- und Karbonatitschmelzen des Shombole-Vulkans, Ostafrika, sind nicht mischbar: Petrographische und experimentelle Ergebnisse

Wir fassen die Hinweise auf fehlende Mischbarkeit von Silikat-Karbonatschmelzen in zwei Nephelinitlaven des Shombole-Vulkans, Ostafrika, zusammen und diskutieren die Bedeutung der Ergebnisse für die Genese der Karbonatite. Die Nephelinitlaven enthalten rundliche bis unregelmäßig geformte Einschlüsse von bis zu 0,5 cm Durchmesser, die Sr-armen Kalzit, Sr–Ca und K–Ba Zeolite, Fluorit, Aegirin, Strontianit und Fluorapatit enthalten. Diese Einschlüsse ("Globules") sind magmatischen Ursprungs und stellen rasch abgekühlte unmischbare Karbonat-Schmelze dar. Die meisten Phasen in den Einschlüssen bilden ein vernetztes Mosaik idiomorpher Kristalle. Selten kommen auch tröpfchenförmige Verwachsungen von Kalzit und Strontianit vor, die auf eutektische Kristallisation aus einer Schmelze hinweisen. Die Assoziationen der Phasen, und die Zuammensetzungen der Minerale in den Einschlüssen und in der silikatischen Grundmasse sind fast identisch, und weisen darauf hin, daß die Proben rasch abgekühlt wurden als beide Schmelzen beinahe im Gleichgewicht waren. Experimente mit den Proben bei 200–500 MPa und 975–925 °C haben die natürlichen Assoziationen (idiomorphe Kristalle und zwei Schmelzen) genau wiedergegeben und Zusammensetzungen der experimentell hergestellten festen Phasen stimmen sehr gut mit denen der ursprünglichen idiomorphen Kristalle überein. Die natürlichen und die experimentell hergestellten Karbonatite sind sövitischer Zuammensetzung (Kalzit-Karbonatit).

Die experimentellen Daten vom Shombole werden mit den bei 300 MPa durchgeführten experimentellen Daten von *Freestone* und *Hamilton* (1980) und *Hamilton* et al. (1989) verglichen; letztere benützten stark peralkalische Gesamtzusammensetzungen die typisch für die Laven des Oldoinyo Lengai-Vulkans sind. Beide Datengruppen sind beinahe koplanar in den Tetraedern Si–(Ca + Mg + Fe^{+2})–(Al + Fe^{+3})–(Na + K) (SCAN), aber die Konoden haben verschiedene Orientierungen und die Oldoinyo Lengai-Zusammensetzungen erzeugen alkalireiche karbonatitische Schmelzen und nicht sövitische. In beiden vulkanischen Zentren ist nur ein Typ von Karbonatiten bekannt und Fraktionierungs-Mechanismen, die einen Karbonatit aus dem anderen ableiten könnten, werden von den erarbeiteten Daten nicht gestützt. Experimente zeigen, daß das volle Spektrum möglicher Ca–Mg(Na + K) Karbonatite durch Unmischbarkeit (immiscibility) aus nephelinitischen Magmen verschiedener Zusammensetzung abgeleitet werden kann.

Introduction

Carbonatites are known to occur on every continent except Antarctica as minor intrusive bodies (dikes, sills, breccias, and small plutons ≤ 5 km^3) and extrusive rocks (lavas, tuffs, and agglomerates) (*Barker*, 1989). They are usually associated in time and space with nephelinites, phonolites, and melilite-bearing rocks and their intrusive equivalents. Most volcanoes which erupt carbonatite are less than 10 km in diameter (e.g. Oldoinyo Lengai, Tanzania: *Dawson*, 1962; Shombole, Kenya: *Peterson*, 1989a), but large nephelinitic stratovolcanoes 50–100 km across

with associated carbonatite dikes or extrusive rocks are known (e.g. the Kaiserstuhl, W. Germany: *Keller*, 1981; Mount Elgon, Uganda: *King* and *Sutherland*, 1966). Most carbonatites are calcic (sövite, alvikite) or magnesian (rauhaugite, beforsite). Alkali-rich carbonatite (natrocarbonatite) has been found only at Oldoinyo Lengai, where it occurs as ash falls and as magma in a periodically active lava lake (*Javoy* et al., 1988; *Dawson*, 1989; *Keller* and *Krafft*, 1990). Older Ca-rich pyroclastic carbonatites have been interpreted as calcified natrocarbonatite (*Hay*, 1983; *Deans* and *Roberts*, 1984), but this interpretation has been questioned by *Keller* (1989) and *Peterson* (1990).

Carbonatites are considered by many to originate by liquid immiscibility at crustal pressures, with the conjugate silicate lavas thought to be mainly nephelinites or phonolites (e.g. *Hamilton* et al., 1979; *Freestone* and *Hamilton*, 1980; *Le Bas*, 1987, 1989). Until recently, experimental evidence for silicate/carbonate liquid immiscibility was restricted to alkali-rich systems and natrocarbonatite (*Koster van Groos* and *Wyllie*, 1966, 1968, 1973; *Verwoerd*, 1978; *Wendlandt* and *Harrison*, 1979; *Freestone* and *Hamilton*, 1980), but *Kjarsgaard* and *Hamilton* (1988, 1989a, b, c) report that immiscibility is also displayed in some Ca-rich systems. A mantle origin for magnesian carbonatites is consistent with the phase equilibria of carbonated peridotite (*Eggler*, 1978; *Wyllie*, 1978; *Wallace* and *Green*, 1989). However, *Eggler* (1989) contends that very few carbonatites have Mg numbers and Ni contents appropriate for mantle-derived magmas. Furthermore, the close association between carbonatites and alkaline ultrabasic rocks (and their derivatives) strongly implies that carbonatites separated from silicate magmas at some point in their evolution, probably during cooling at lower to upper crustal levels (*Barker*, 1989; *Le Bas*, 1989).

At Shombole, an extinct nephelinite-carbonatite volcano on the Kenya-Tanzania border (Fig. 1), sövite occurs as tuffs, dikes, and intrusive breccias associated with nephelinite and phonolite flows and pyroclastic rocks. Many of the nephelinites contain globular segregations rich in carbonates, interpreted by *Peterson* (1989a) as immiscible melt droplets. Experiments by *Kjarsgaard* and *Hamilton* (1989b) on Shombole nephelinites produced silicate-carbonate (nephelinite/sövite and phonolite/sövite) liquid immiscibility together with natural phenocryst assemblages (mostly nepheline + clinopyroxene + Ti-bearing phase). In this paper, we summarize the petrographic and experimental evidence for liquid immiscibility in the Shombole lavas and discuss its significance to carbonatite petrogenesis.

Shombole: Geological Summary

Shombole is a strongly eroded volcanic centre which erupted at 2 Ma (*Fairhead* et al., 1972) onto an uplifted erosional surface of Precambrian crystalline basement (*Baker*, 1963). It was probably contemporaneous with extrusion of the Kordjya basalts, and North Kordjya and Ewaso Ngiro trachytes 70 km to the north (*Crossley*, 1979). Pliocene and Quaternary normal faulting dropped Shombole onto the floor of the Kenya rift, where it now separates the basins of Lakes Natron and Magadi (Fig. 1). Quaternary flood trachytes and recent lacustrine sediments cover Shombole's flanks, but gullying by heavy seasonal rains has produced steep-walled exposures of the internal structure. A normal fault cuts across the eastern edge of the central vent area, where flat-lying pyroclastic rocks and minor flows are exposed

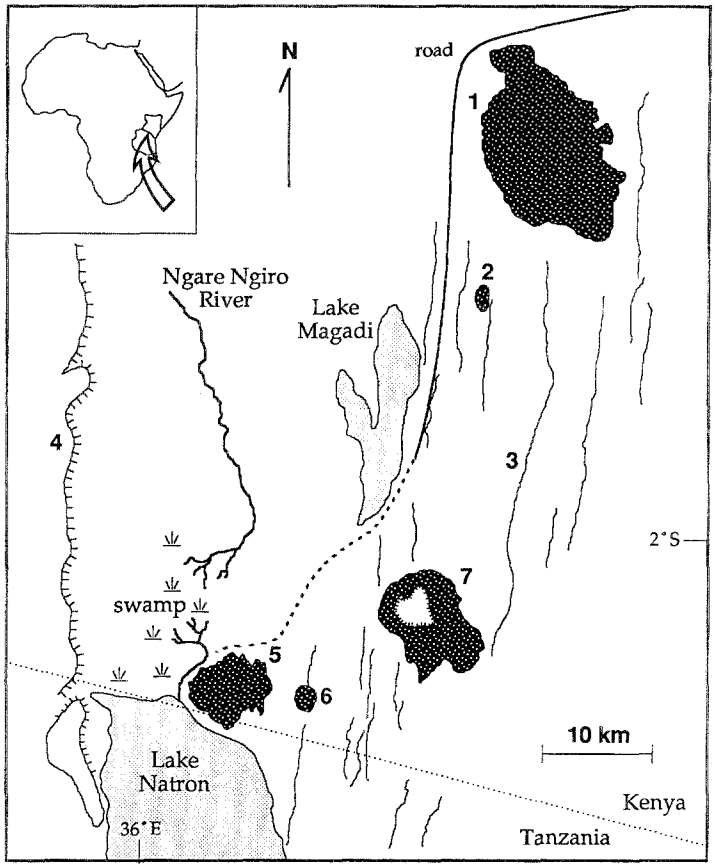

Fig. 1. Geography of the Shombole area (south Kenya/north Tanzania). (*1*) Olorgesalie (basaltic volcano); (*2*) Oldoinyo Nyokie (trachyte dome); (*3*) normal fault trace; (*4*) Ngurumann Escarpment (western rift wall); (*5*) Shombole (nephelinite volcano); (*6*) Oldoinyo Alasho (trachyte dome); (*7*) Lenderut (basaltic volcano/caldera)

in contact with outwardly dipping nephelinite lavas, agglomerates and debris flows. Carbonatites occur as sövite dikes, intrusive breccias, and ash tuffs (*Peterson*, 1989a).

The silicate lavas of Shombole have been described by *Peterson* (1989a). They range from silica-poor nephelinites (40% SiO_2) with perovskite and melanite microphenocrysts, to titanite-bearing and phonolitic nephelinites with groundmass sanidine (48% SiO_2). All contain 20–50 modal percent nepheline + clinopyroxene. Phonolites ($\geq 50\%$ SiO_2) also occur at Shombole. The Nd and Sr isotopic compositions of the nephelinites and carbonatites are indistinguishable, but most of the phonolites must have been contaminated by lower crust (*Bell* and *Peterson*, in press). The phonolite lavas do not contain carbonate globules.

Two globule-bearing nephelinites, SH40 and SH49, were selected for detailed petrographic and experimental study. Sample SH40 is a titanite nephelinite containing phenocrysts of nepheline, aegirine-augite, magnetite, and titanite, together with calcite-rich globules (6%), set in a fine-grained groundmass consisting of nepheline and clinopyroxene with subordinate alkali feldspar (Plate 1). Sample SH49 is a perovskite nephelinite with phenocrysts of nepheline, diopside, and perovskite, with carbonate globules (9%), set in a fine-grained groundmass. Photomicrographs of

Table 1. *Modal mineralogy of Shombole nephelinites SH40 and SH49.* Based on 1000 point counts

Sample	SH49	SH40
groundmass	65.6	53.6
globules	8.9	5.7
nepheline	18.4	24.4
clinopyroxene	5.5	10.6
titanite	0	1.9
perovskite	1.0	0
magnetite	0.2	0.1
apatite	0.3	0
xenoliths	0.1	0
vesicles	0	3.7

SH49 are shown in *Peterson* (1989a) and *Kjarsgaard* and *Hamilton* (1989c). Modal analyses of the samples are given in Table 1.

Petrography and Mineralogy of the Globules

The carbonate globules in both lavas are 0.1 to 5 mm across and have sharply defined contacts with the enclosing groundmass (Plates 1–4). In general, smaller globules are spherical (Plates 3, 4) but larger ones are often irregular due to coalescence with adjoining globules and draping around phenocrysts (Plate 1). Phases found in the globules are, in decreasing order of abundance: calcite, Ca–Sr and K–Ba zeolites, fluorite, aegirine, strontianite, fluorapatite, magnetite, sanidine (SH40 only), and barium lamprophyllite (SH49 only). Representative microprobe

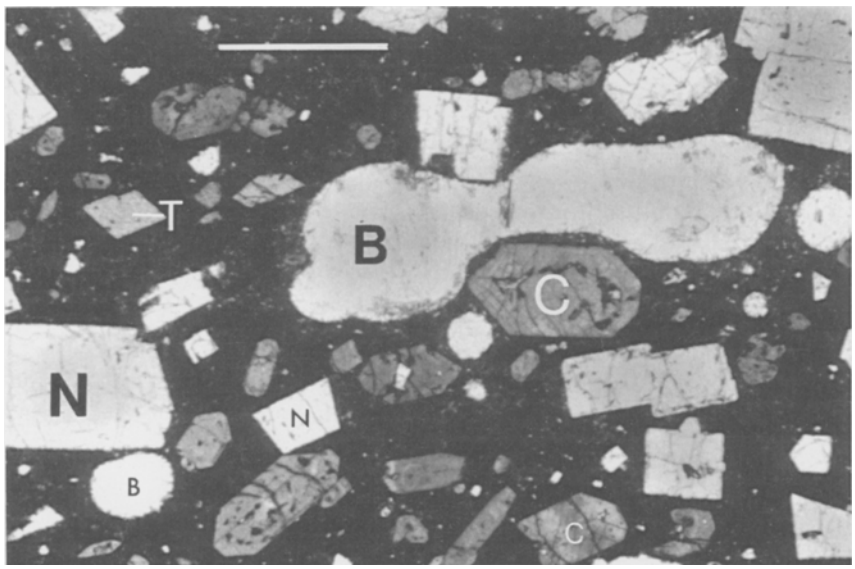

Plate 1. Photomicrograph of sample SH40. *N* nepheline, *C* clinopyroxene, *T* titanite, *B* carbonatite globule. Note small globule coalescing onto the left end of larger globule, which is draped between two phenocrysts. Scale bar = 1.0 mm. Plane polarized light

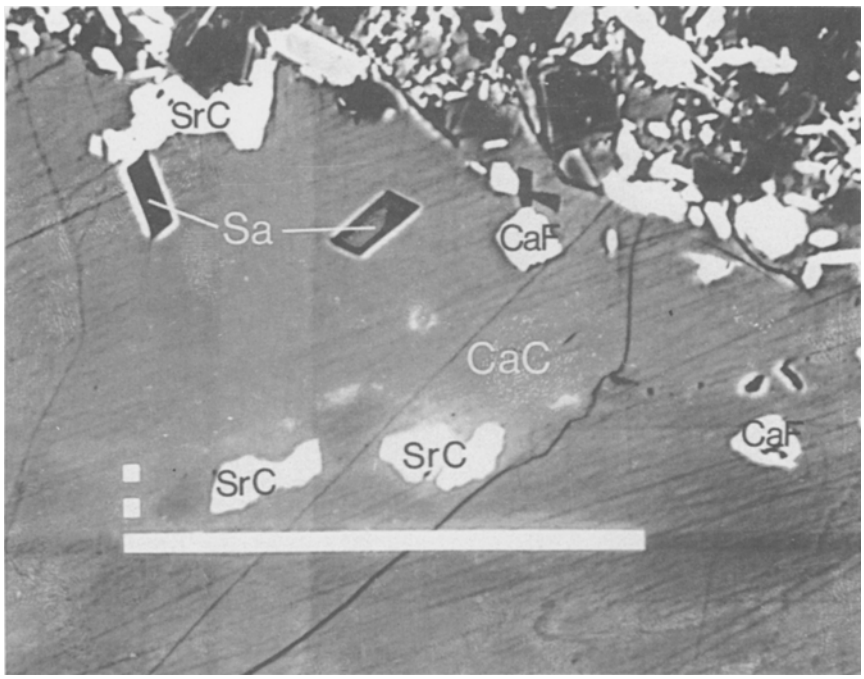

Plate 2. Backscattered electron image of sample SH40. Shown is a carbonate globule, with silicate groundmass in the upper right corner. Tabular sanidine (*Sa*) plus subhedral strontianite (*SrC*) and fluorite (*CaF*) are surrounded by low-Sr calcite (*CaC*). Scale bar = 100 μm

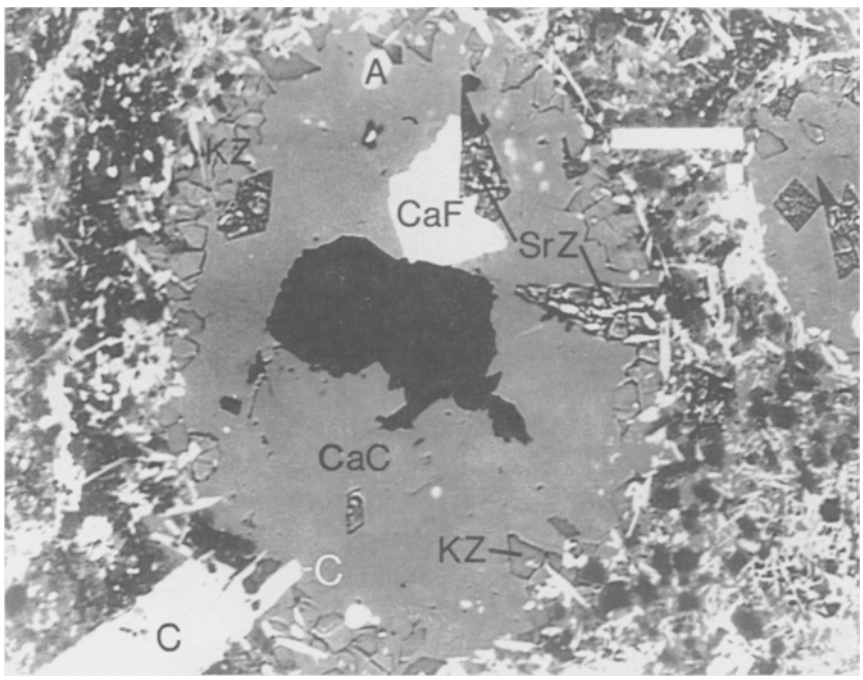

Plate 3. Backscattered electron image of carbonate globules in sample SH49. *A* fluorapatite, *C* clinopyroxene (aegirine-rich); *CaF* fluorite, *CaC* calcite, *SrZ* strontium- and calcium-rich zeolite, *KZ* potassium- and barium-rich zeolite. The hole (black irregular area in middle of globule) was accidentally produced during sample preparation, and may be an enlargement of a (formerly) gas-filled hole in the globule. Scale bar (between the globules) = 500 μm

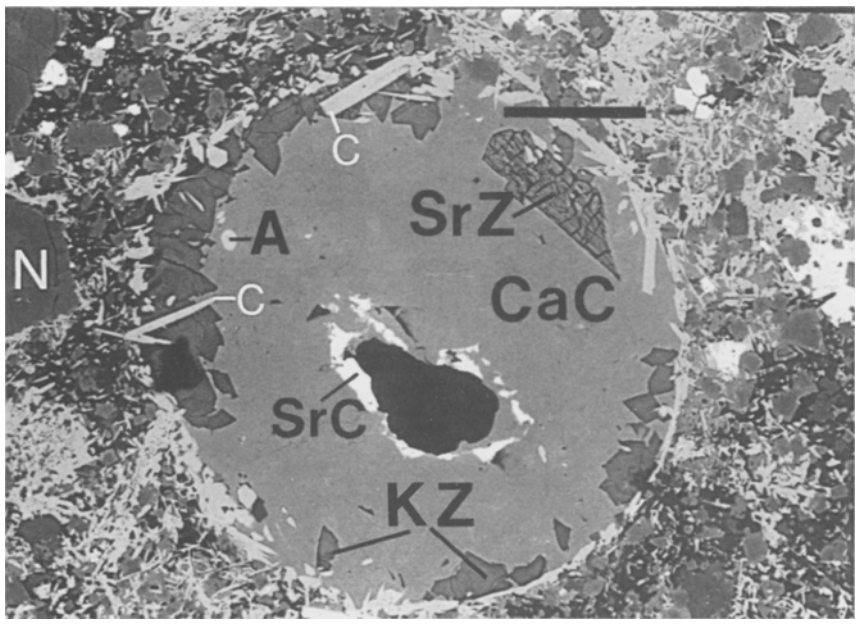

Plate 4. Backscattered electron image of a carbonate globule in sample SH49. Phases labelled as in Plates 2 and 3, plus N = nepheline (phenocryst occurring in the silicate groundmass). Note the projection of acicular pyroxene across the globule interface, demonstrating that it was in equilibrium with both liquids at the time of eruption. Dark region in the centre of the globule with smooth boundaries is interpreted to represent a former gas vesicle. Scale bar = 500 μm (top right side of globule)

analyses are listed in Tables 2 and 3. There is significant substitution of Sr for Ca in apatite, fluorite and calcite.

Magnetite and zeolites nucleated mainly on the globule-groundmass interface, but 'free-floating' euhedra of zeolites, aegirine, fluorite, and apatite are common (Plates 2–4). Acicular aegirine and tabular sanidine occasionally cut across the silicate/carbonate meniscus (Plate 4). Strontianite usually occurs as subhedral to euhedral crystals (Plates 2, 4), but also as blebby intergrowths with low-Sr calcite. These latter textures are similar to those observed between gregoryite, witherite, and KCl in the groundmass of natrocarbonatite, and interpreted as a product of eutectic crystallization (*Peterson*, 1990). The shapes and internal textures of the globules are consistent with precipitation of solid phases from a melt (an interlocking mosaic of minerals is observed). Holes with smooth, spherical boundaries within some of the carbonate melt droplets are interpreted to indicate the former existence of gas bubbles (Plate 4).

The mineralogy of the globules satisfies the conditions for equilibrium liquid immiscibility. With the exception of nepheline, phases present in the silicate groundmass are, in general, also present in the globules. The compositions of clinopyroxene, sanidine, and apatite in the groundmass are nearly identical to those in the globules (c.f. Table 3). The absence of nepheline in the carbonate globules is problematic. The possibility that immiscibility occurred only prior to nepheline saturation, or that the nepheline in the globules was replaced by zeolites is inconsistent with textural evidence. The lavas are fresh, and show no evidence of post-eruption alteration

Table 2. *Electron microprobe analyses of phases in the carbonate globules from SH8, SH40 and SH49*

Phase	fluorite	calcite	stront	Sr-Ca zeo	K-Ba zeo	mag	Ba-lamp	glass
Sample	SH49	SH40	SH40	SH49	SH49	SH49	SH49	SH8
SiO_2	0.00	0.00	0.00	51.11	60.07	0.53	31.22	52.69
TiO_2	0.00	0.00	0.00	0.02	0.07	4.60	24.09	0.72
Al_2O_3	0.00	0.00	0.00	23.02	17.95	0.06	0.44	20.43
FeO_t	0.00	0.07	0.00	0.82	0.96	78.86	1.65	3.47
MnO	0.00	0.00	0.00	0.01	0.03	4.19	0.55	0.21
MgO	0.00	0.04	0.02	0.01	0.01	0.63	1.55	0.35
CaO	49.67*	54.44	9.85	6.38	3.49	1.87	3.50	2.25
SrO	0.30*	0.39	57.74	6.66	0.04	n.a.	3.12	n.a.
BaO	0.00	0.09	1.07	0.26	1.86	n.a.	24.94	n.a.
Na_2O	0.00	0.00	0.00	0.19	1.34	0.75	8.02	8.86
K_2O	0.00	0.00	0.00	0.63	7.86	n.a.	1.87	0.54
SUM	102.41*	55.30	68.71	89.11	93.68	90.99	102.54#	89.87¤

stront = strontianite; Sr–Ca zeo = strontium- and calcium-rich zeolite; K–Ba zeo = potassium- and barium-rich zeolite; mag = magnetite; Ba-lamp = barium lamprophyllite. * = values are elemental, not oxide, SUM includes 52.44% F; # = SUM includes 2.74 wt% F, corrected for O ≡ F; ¤ = SUM includes 0.35% P_2O_5; n.a. = not analysed. Analyses performed at the Geological Survey of Canada, Ottawa; all elements determined by wavelength dispersive techniques.

Table 3. *Electron microprobe analyses of solid phases in the carbonate globules and the silicate groundmass (g/mass)* of samples SH40 and SH49

Phase	CPX	CPX	CPX	CPX	SAN	SAN	AP	AP
Sample	SH49	SH49	SH40	SH40	SH40	SH40	SH49	SH49
Type	globule	g/mass	globule	g/mass	globule	g/mass	globule	g/mass
SiO_2	50.79	51.10	52.25	52.66	66.07	65.45	0.00	0.00
TiO_2	1.34	0.87	1.55	1.67	0.00	0.00	0.00	0.00
Al_2O_3	0.30	0.22	0.51	0.79	16.95	17.12	0.00	0.00
FeO_t	27.85	28.84	25.91	24.69	1.63	1.55	0.34	0.36
MnO	0.27	0.23	0.83	0.49	0.00	0.00	0.01	0.00
MgO	1.20	1.08	1.75	2.05	0.00	0.00	0.06	0.00
CaO	4.85	3.83	4.91	4.81	0.00	0.04	49.19	49.93
SrO	n.a.	n.a.	n.a.	n.a.	0.00	0.00	3.02	3.14
BaO	n.a.	n.a.	n.a.	n.a.	1.12	1.88	0.09	0.08
Na_2O	12.89	12.49	12.56	11.55	1.51	1.52	n.a.	n.a.
K_2O	n.a.	n.a.	n.a.	n.a.	14.48	14.19	n.a.	n.a.
P_2O_5	n.a.	n.a.	n.a.	n.a.	n.a.	n.a.	36.49	35.51
F	n.a.	n.a.	n.a.	n.a.	n.a.	n.a.	3.67	3.70
SUM	99.49	98.66	100.27	98.71	101.35	102.01	91.30*	91.16*

CPX = clinopyroxene; SAN = sanidine; AP = apatite. Pyroxene and sanidine analyses performed at the Geological Survey of Canada, Ottawa; all elements determined by wavelength dispersive techniques. Apatite analyses performed at the University of Manchester; SrO, BaO and F determined by wavelength dispersive techniques, all other elements by energy dispersive techniques. * = SUM corrected for O ≡ F; n.a. = not analysed.

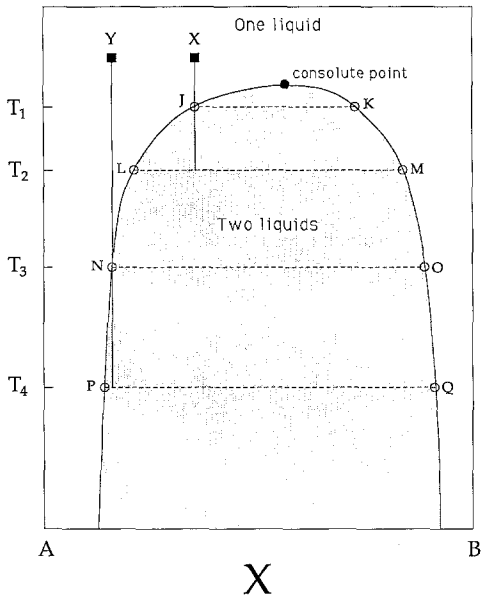

Fig. 2. T–X diagram illustrating a hypothetical binary system with two-liquid field. The liquidus has been omitted for clarity since the one-liquid/two-liquid field boundary is dependant only on melt composition, and is independant of the presence or absence of solid phases (*Roedder*, 1979). By comparing compositions *X* and *Y*(filled squares), it can be seen that under conditions of non-equilibrium cooling, the steepness of the solvus limbs are critical as to the degree to which compound immiscibility occurs. Composition *X*, with cooling intersects the two-liquid solvus at T_1, near the consolute point. At T_1 two liquids, *J* (a liquid rich in *A*) and *K* (a liquid rich in *B*) are in equilibrium. With cooling from T_1 to T_2, *J* follows the solvus limb *JL*, and exsolves a B-rich second liquid whose changing composition lies between *KM*. Using the lever rule, *X* exsolves about 23% of B-rich liquid *M* in cooling from T_1 to T_2. In comparison, composition *Y* intersects the two-liquid solvus at T_3, were the solvus limbs are relatively steep. At T_3, two liquids, *N* and *O* are in equilibrium. With cooling from T_3 to T_4, *E* follows the solvus limb *EG*, exsolving a B-rich liquid whose changing composition lies between *OQ*. Liquid *N* exsolves about 2% of B-rich liquid *Q* in cooling from T_3 to T_4. For composition *Y*, if it represented a natural system, observing compound immiscibility would be quite difficult due to the small proportion of second liquid exsolved. Note that under conditions of perfect equilibrium cooling, compound immiscibility does not occur

(*Peterson*, 1989a). Zeolite compositions are low in sodium (<1.5 wt% Na_2O) and either K and Ba- or Sr and Ca-rich, suggesting they are probably not replacing nepheline.

Compound immiscibility, produced by further widening of the solvus after initial two-liquid separation, should result in globules forming within globules under non-equilibrium cooling conditions, provided the solvus limbs are not too steep (*Bowen*, 1928; see Fig. 2). Compound immiscibility was not observed in SH40 or SH49, but this is consistent with either steep solvus limbs and/or the carbonate globules remaining in equilibrium with their nephelinitic host. However, another nephelinite (SH8: Plate 5) contains globules with evidence of three preserved liquids: a core of zeolite + carbonate, surrounded by a rim of yellow-brown glass containing tiny (1 μm) spheres of Fe-rich sulphides. The glass, partially devitrified

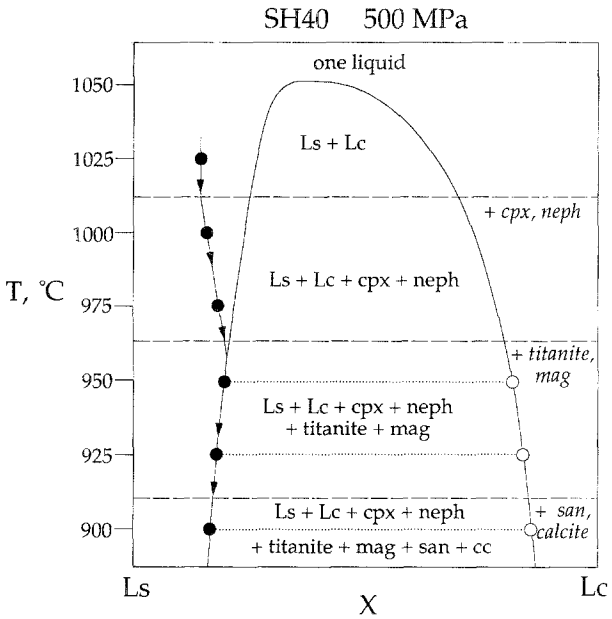

Fig. 3. Experimentally determined schematic T–X diagram for sample SH40 at 500 MPa; *Ls* silicate liquid, *Lc* carbonate liquid, *cpx* clinopyroxene, *neph* nepheline, *mag* magnetite, *san* sanidine, *cc* calcite. Circles correspond to individual runs. Dashed lines indicate the appearance of solid phases on the liquidus. Silicate liquids are indicated by filled circles, carbonate liquids by open circles. Conjugate liquid pairs joined by dotted lines. The shape and closure temperature of the two-liquid field is based on all Shombole experiments (SH40, SH49, and SH49 + 10 wt% calcite). At 1025 °C the starting composition is in the one liquid field. Clinopyroxene and nepheline start to precipitate at about 1015 °C, which increases the carbonate component in the residual silicate liquid. The two-liquid field is intersected, and titanite plus magnetite appear as liquidus phases at 960 °C (which duplicates the phase assemblage of the starting materials). Calcite and sanidine appear on the liquidus at about 915 °C

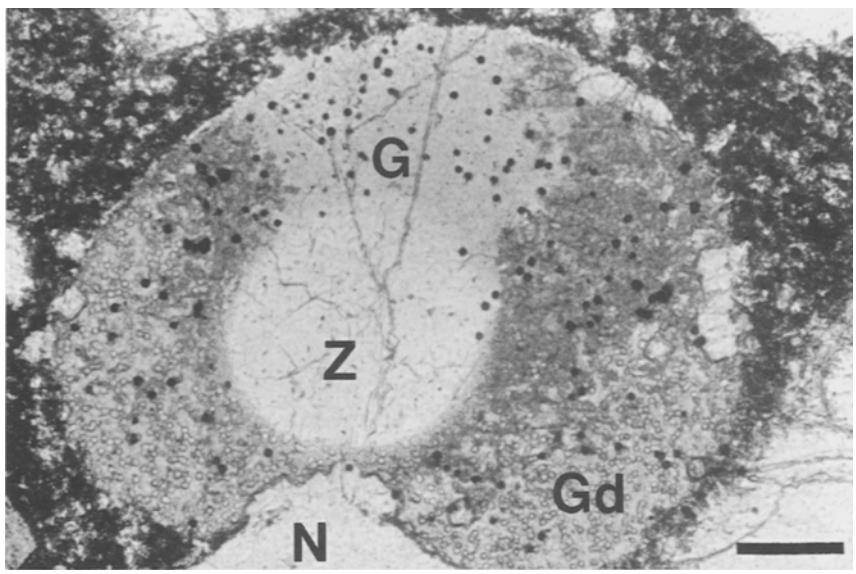

Plate 5. Photomicrograph of sample SH8 a compound immiscible globule. *Z* zeolite-carbonate; *G* CO_2-rich phonolitic glass; *Gd* devitrified glass. Note the presence of minute (≤ 1 μm) opaque spheres of Fe–Mn sulphides in the phonolitic glass (*G*), and its partial devitrification to carbonates (*Gd*). Plane polarized light. Scale bar = 100 μm

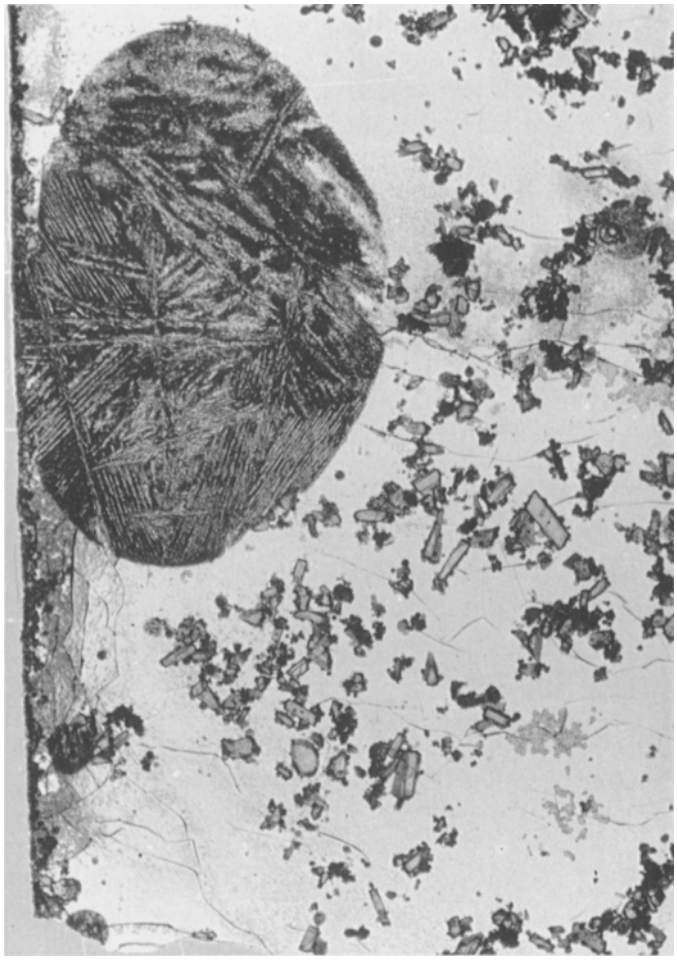

Plate 6. Photomicrograph of experimental run BK208 (starting composition = SH49 + 10 wt% $CaCO_3$). Run conditions were 500 MPa and 1000 °C. One large (long axis 2 mm) and numerous small (50–100 μm) spheroids of low-alkali (9 wt% $Na_2O + K_2O$) carbonate liquid that have quenched to dendritic intergrowths are surrounded by silicate glass. The dendrites are low-Sr calcite, with the areas between consisting of microcrystalline aggregates rich in Na, K, Fe, Mg, Sr, Ba, F, Cl, Si and Al. Crystals in the glass are all of clinopyroxene. Note that many of the clinopyroxenes are partly surrounded by small immiscible carbonate spheres, possibly indicating preferential nucleation at the two-liquid interface. Plane polarized light

to carbonates, has a volatile-rich phonolitic composition (Table 2). The textures in sample SH8 can be interpreted as being produced by the following sequence: (1) intersection of the two-liquid solvus near the consolute point, where the exsolved carbonate liquid has a high silicate liquid component, (2) non-equilibrium cooling, to generate the observed compound zeolite-carbonate and volatile-rich phonolitic liquids, (3) exsolution of a sulphide liquid from the phonolitic melt, possibly induced by further cooling or by loss of $CO_2 + H_2O$ via partitioning into the carbonatite liquid and/or fluid phase. No sulphide spheres are found in the core of the globules, consistent with the higher solubility of sulphur species in carbonate liquids as compared to alkali-silicate liquids (*Helz* and *Wyllie*, 1979; *Wyllie*, 1989).

Since compound immiscibility was not observed in the other samples, we suggest that most of the Shombole nephelinite magmas intersected the two-liquid solvus at temperatures significantly lower than the consolute point, where the solvus limbs are steep (c.f. Fig. 2 and 3, and below). Furthermore, as solid phases in the globules have compositions similar to those in the groundmass, this suggests that the immiscible globules remained in equilibrium with their nephelinitic host during differentiation.

As previously noted, textural and chemical evidence are not supportive of a secondary origin for the zeolites. Additionally, the occurrence of zeolites in the globules does not necessarily suggest high H_2O content in the carbonate liquid. *Kim* and *Burley* (1971) have illustrated that analcime can precipitate in H_2O-undersaturated silicate melts in the P–T range 515–1250 MPa and 575–657 °C, and on this basis we see no reason for differences with H_2O-undersaturated carbonate melts. A minimum of 1.5 wt% H_2O in the immiscible carbonate liquids is suggested on the basis that the globules contain about 15 modal% zeolites (containing 10 wt% H_2O).

Gittins (1988) has emphasized that carbonate globules purported to be carbonatite should contain minerals consistent with the known high concentration of certain trace elements in carbonatites. It is clear that the phase assemblage of the globules (calcite plus fluorite, fluorapatite, strontianite, barium lamprophyllite and Sr- and Ba-bearing zeolites) is consistent with this requirement.

Experimental Study of Immiscibility

Experiments were performed in internally heated pressure vessels at pressures of 200–500 MPa, with gold tubing as a sample container. Ground rock powders of Shombole SH40, SH49 and SH49 + 10 wt% $CaCO_3$ were used as starting materials. Details of experimental techniques are in *Kjarsgaard* and *Hamilton* (1988) and *Freestone* and *Hamilton* (1980). Runs were brought directly to run temperature, as problems with preferential nucleation of high Ti–Al clinopyroxenes occurred with reversal type experiments (*Kjarsgaard*, 1990). As noted by *Twyman* and *Gittins* (1987) and *Gittins* (1988, 1989), the one-liquid/two-liquid field boundary was not specifically determined in previous experimental studies, which seriously compromises the viability of the immiscibility hypothesis. The one liquid ± crystals field was located for all of the bulk compositions in this study. Complete listings of experimental conditions, assemblages, and compositions will be given elsewhere (*Kjarsgaard* and *Hamilton*, in prep.).

The carbonate globules in the experiments are homogeneous polycrystalline spheres up to 2.0 mm wide (Plate 6). Globules, solid phases, and silicate glasses were analyzed by electron microprobe. Solid phases in equilibrium with two liquids (clinopyroxene, nepheline, melanite, perovskite, titanite, magnetite and sanidine) correlate very well with the natural assemblages and have compositions nearly identical to phenocrysts in the lavas (see Table 4). The crystallization of sample SH40 is traced in a schematic silicate-carbonate pseudobinary T–X diagram in Fig. 3. At 500 MPa, clinopyroxene and nepheline crystallize from one liquid at about 1015 °C. The two-liquid field is intersected by 950 °C, at which point titanite and magnetite appear on the liquidus, thus reproducing the phase assemblage of the lava. With further cooling, sanidine and calcite are stable liquidus phases (915 °C).

Assuming that the experiments closely model the magmatic conditions, the temperature at solvus intersection (ca. 960 °C at 500 MPa) is a maximum for the eruption temperature of SH40, since the liquid composition must lie on the silicate limb of the two-liquid field. This is consistent with nepheline-liquid geothermometry (*Peterson*, 1989a) which indicated an eruption temperature for SH40 of 840 °C. A slightly more basic titanite nephelinite (sample SH62) gave a temperature of 950 °C; this sample contains very few globules (< 0.1%) which quenched to a yellow-brown glass similar to that in SH8, as described above. The temperature at which the solvus

Table 4. *Electron microprobe analyses of solid phases in selected experimental charges (starting composition = SH40)* and in natural sample SH40

Sample	BK292[1]	BK339[2]	SH40	BK344[3]	BK292[1]	SH40	SH40
Phase	neph	neph	neph	CPX	CPX	CPX	CPX
Type	EC	EC	P	EC	EC	PC	PR
SiO_2	44.89	42.04	43.59	49.69	48.26	50.32	49.25
TiO_2	n.a.	n.a.	n.a.	1.04	0.79	0.83	0.82
Al_2O_3	30.92	33.36	31.30	1.53	0.84	1.26	1.07
Fe_2O_3	2.12	1.81	2.41	n.a.	n.a.	n.a.	n.a.
FeO_t	n.a.	n.a.	n.a.	14.59	18.80	15.07	18.66
MnO	n.a.	n.a.	n.a.	0.60	0.63	0.54	0.57
MgO	n.a.	n.a.	n.a.	8.20	6.30	9.24	6.88
CaO	0.39	0.46	0.18	21.48	18.80	21.27	18.66
Na_2O	16.63	16.22	16.86	2.49	3.16	1.95	3.34
K_2O	4.69	5.45	5.52	n.a.	n.a.	n.a.	n.a.
SUM	99.08	99.34	99.86	99.62	97.59	100.48	99.25

Experimental conditions: (1) 500 MPa, 925 °C; (2) 200 MPa, 925 °C; (3) 500 MPa, 975 °C. EC = experimental charge; P = phenocryst; PC = phenocryst core; PR = phenocryst rim; n.a. = not analysed. Analyses performed at the University of Manchester; all elements determined by energy dispersive techniques.

is intersected will be a function of CO_2 content, bulk composition, and pressure, and it is not surprising that a variety of textures and compositions for the globules in the nephelinites is observed.

A more quantitative projection of the two-liquid solvus can be made in the CO_2 saturated quaternary Si–(Ca + Mg + Fe^{2+})–(Al + Fe^{3+})–(Na + K)(SCAN). This diagram separates carbonates from silicates and (Na + K)-rich carbonatites from Ca-rich carbonatites. It also discriminates silicate magma compositions on the basis of their peralkalinity. Silicate and carbonate liquid $Fe^{3+}/(Fe^{2+} + Fe^{3+})$ ratios for the experimental liquids were determined from analysed FeO_t and the equations of *Sack* et al. (1980), with f_{O_2} = NNO. Since these equations were calibrated for silicate liquids, the calculated ratios for the carbonate liquids are highly uncertain. The calculated $Fe^{3+}/(Fe^{2+} + Fe^{3+})$ ratios for carbonatite liquids are high, ranging from 0.61 to 0.93.

The compositions of liquids generated by experiments at 500 MPa on Shombole nephelinites are plotted in SCAN in Fig. 4. A plane fit by least squares to the data has nearly constant Si/(Si + Al + Fe^{3+}) of 0.70, and the data points all cluster very closely to this plane. The silicate liquids lie near the nepheline-diopside join, appropriate for nephelinites. The alkali content of both silicate and conjugate carbonate liquids increases with falling temperature, due to concentration of Na + K through precipitation of mafic minerals.

In Fig. 5a, the Shombole two-liquid tielines have been extended to intersect the Si–(Al + Fe^{3+})–(Na + K)(SAN) plane. The intersection of extended tielines with the SAN plane defines a limited area which is slightly more silica-rich than the composition of stoichiometric nepheline, and partly lies within the 1 atm liquidus field of nepheline (Fig. 5b). Figures 5a and b provide a possible explanation for the

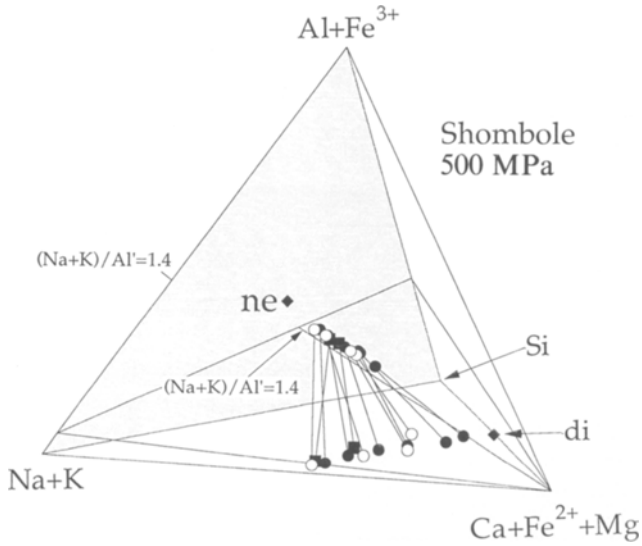

Fig. 4. Projections of experimental 500 MPa Shombole silicate and carbonate liquids onto the CO_2 saturated Si–(Ca + Mg + Fe^{2+})–(Al + Fe^{3+})–(Na + K) (SCAN) quaternary. The carbonate liquids plot closest to the C–N edge, and tielines join conjugate silicate and carbonate liquids of individual runs. The intersections of planes fit by least squares to the data are indicated by solid lines on the faces of the tetrahedron. The intersections of these planes with the constant peralkalinity plane (Na + K)/Al′ = 1.4 (Al′ = Al + Fe^{3+}) are indicated by a dashed line, and one apex of the peralkalinity plane is indicated on the N–A edge. Stoichiometric nepheline (*ne*) and diopside (*di*) are indicated by filled diamonds. Shombole starting materials: squares = SH40; open circles = SH49; filled circles = SH49 + 10 wt% calcite. Data are plotted in atomic %

absence of nepheline in the carbonate globules, by utilizing the extended tie line rule of *Roedder* (1979, page 20; and pers. comm.). Shombole tielines, extended to the SAN plane do not converge on the composition point of natural or stoichiometric nepheline, but this may be a result of our ferrous—ferric recalculation and/or projection techniques. However, the general geometry of the phase relations is still consistent with nepheline precipitating only in the silicate liquid. In SCAN quaternary space, the liquidus volume of nepheline closes away from the SAN plane towards Ca + Mg + Fe^{2+}, and intersects only the silicate limb of the solvus, not the carbonate limb (which is Ca-, Mg- and Fe^{2+}-rich). With cooling, a carbonated silicate liquid precipitates solid phases and exsolves an immiscible carbonatite liquid, however, nepheline (which is in equilibrium with both liquids) precipitates only in the silicate liquid.

In Fig. 6 the 300 MPa two-liquid data for the experiments of *Freestone* and *Hamilton* (1980) and *Hamilton* et al. (1989) are plotted. The bulk compositions for these experiments were mixtures of either nephelinite or phonolite from Oldoinyo Lengai, with synthetic carbonatites of natrocarbonatite or high-alkali sövite composition. The least-squares fit plane has an orientation nearly identical to that calculated for the Shombole data.

The two data sets differ in that the silicate and carbonate liquids generated using Shombole rocks as starting materials are substantially less alkaline; immiscible Shombole carbonate liquids have 4–16 wt% $Na_2O + K_2O$, and correspond to

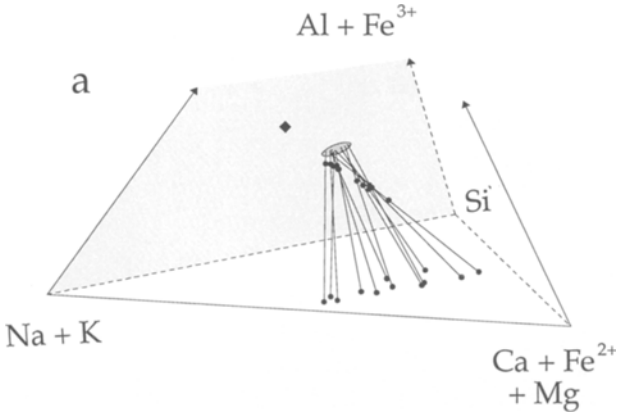

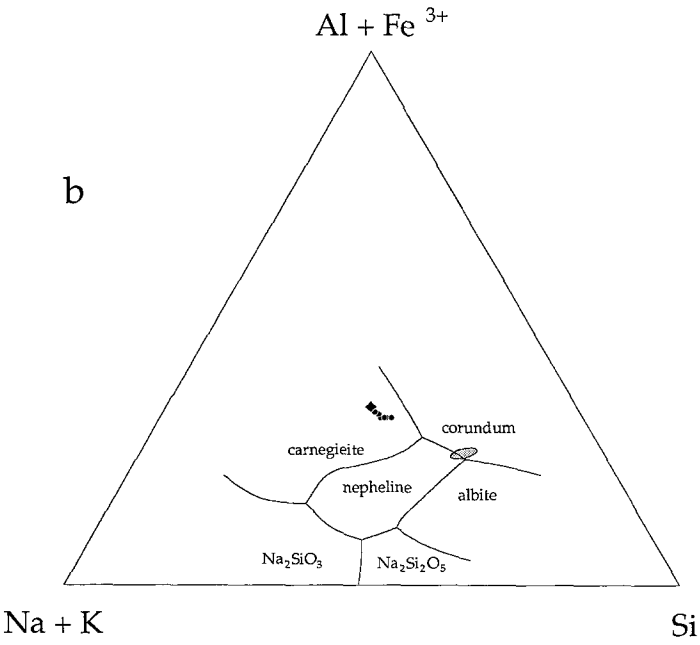

Fig. 5. (a) Shombole two-liquid tie lines in SCAN extended to their intersection with the SAN plane. Stoichiometric nepheline (ne) indicated by a filled diamond. (b) Intersection of extended tie lines with the SAN plane (shaded oval). Stoichiometric nepheline (ne) indicated by a filled diamond, Shombole nepheline phenocrysts indicated by filled circles. Field boundaries for the system Na_2O–Al_2O_3–SiO_2 at 1 atm from Levin et al. (1964), see text for further details. Data for Fig. 5a and b plotted in atomic %

low-alkali sövite, whereas immiscible Lengai carbonate liquids have 17–36 wt% $Na_2O + K_2O$, and correspond to high-alkali sövite/natrocarbonatite. With reference to the Na_2CO_3–K_2CO_3–$CaCO_3$ ternary (*Cooper* et al., 1975), the experimental Shombole carbonate liquids all plot within the liquidus field of calcite, whereas the majority of the Lengai carbonate liquids plot within the nyerereite liquidus field (see Fig. 7). Most of the experimentally produced Lengai liquids with cooling will precipitate nyerereite and gregoryite, the two Na–K–Ca carbonate phases which are prominent phenocrysts in natural natrocarbonatite.

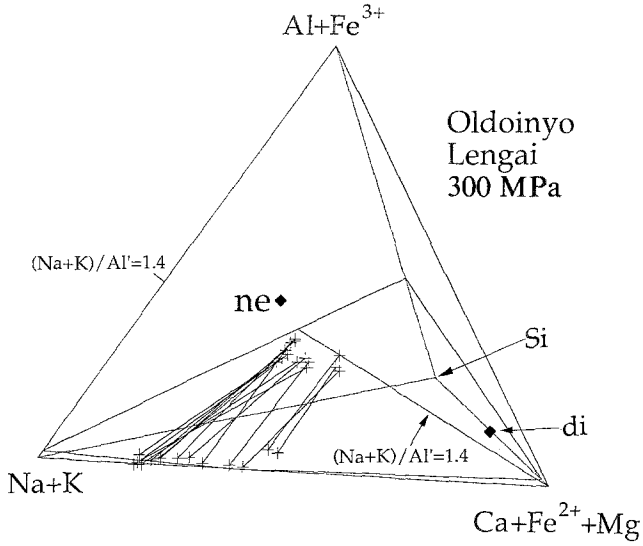

Fig. 6. Projections of experimental Oldoinyo Lengai silicate and carbonate liquids onto SCAN. Data from *Freestone* and *Hamilton* (1980) and *Hamilton* et al. (1989). All other symbols as per Fig. 4. Data are plotted in atomic %

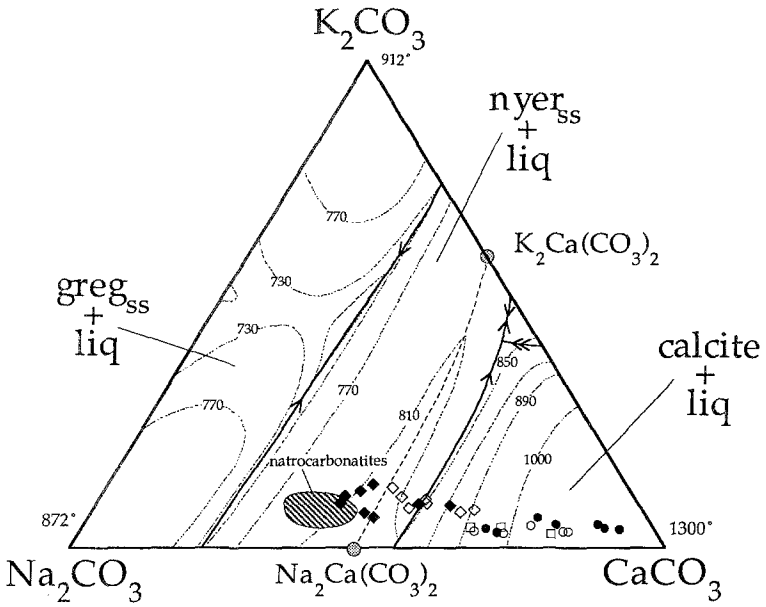

Fig. 7. Plot of immiscible carbonate liquids from Shombole (500 MPa) and Oldoinyo Lengai (300 MPa) experiments onto the ternary $CaCO_3$–Na_2CO_3–K_2CO_3 100 MPa liquidus diagram of *Cooper* et al. (1975). Symbols: filled diamonds, Oldoinyo Lengai phonolite system; open diamonds, Oldoinyo Lengai nephelinite system (data from *Freestone* and *Hamilton*, 1980 and *Hamilton* et al., 1989); filled circles, Shombole SH49 + 10 wt% $CaCO_3$; open circles, Shombole SH49; open squares, Shombole SH40 (all this study). The shaded area labelled natrocarbonatite is from *Peterson* (1990). Data are plotted in wt%

The experimental Shombole silicate liquids all plot above the plane (Na + K)/Al′ = 1.4 (where Al′ = Al + Fe^{3+}), whereas the Lengai silicate liquids all plot below it, i.e., the bulk compositions of the experiments based on Lengai starting materials

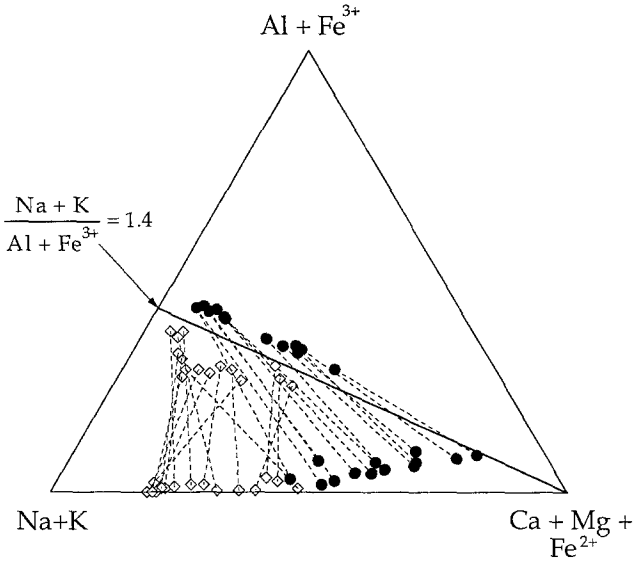

Fig. 8. Projection from Si of experimentally determined Shombole and Oldoinyo Lengai tie lines onto the plane (Ca + Mg + Fe^{2+})–(Al + Fe^{3+})–(Na + K) to illustrate the effect of silicate liquid peralkalinity on exsolved carbonate liquid composition. Symbols: filled circles, 500 MPa Shombole SH40, SH49, SH49 + 10 wt% $CaCO_3$ (all this study); open diamonds, 300 MPa Oldoinyo Lengai nephelinite and phonolite systems (*Freestone* and *Hamilton*, 1980 and *Hamilton* et al., 1989). See text for details. Data are plotted in atomic %

are much more peralkaline. *Freestone* and *Hamilton* (1980) illustrated a widening of the solvus with increasing pressure for the Lengai system. At 200–500 MPa the Shombole two-liquid field does not show this pressure effect (*Kjarsgaard* 1990; *Kjarsgaard* and *Hamilton*, in prep.) . We therefore consider that the peralkalinity contrast is primarily responsible for the differences between the two systems (see Fig. 8). However, we note that the mass fraction of carbonatite in the Lengai-based experiments is much higher (up to 45%; due to the starting mixtures used) than in the Shombole-based experiments, where whole CO_2-nephelinites plus 0–10% $CaCO_3$ were used as starting materials. The Lengai runs consequently are saturated with carbonate liquid at much higher temperatures (up to 1250 °C!). However, temperature appears to have a negligible effect on tieline orientation (Fig. 8 of *Freestone* and *Hamilton*, 1980). It is not possible to assess the roles of varying Na/(Na + K), Si/Si + Al, or Ca/(Ca + Mg + Fe^{2+}) with the data presently available. Further experiments, particularly with more Mg-rich bulk compositions, are required before the P–T–X controls on exsolved carbonate liquid composition can be fully understood.

Discussion

There has been a long-standing debate concerning the origin, or even the existence, of sövite magma. This has been summarized elsewhere (*Keller*, 1989; *Wyllie*, 1989; *Peterson*, 1989b, 1990). We will note here only that the recent identification and description of fresh, juvenile sövite lavas and agglomerates (e.g. *Keller*, 1981, 1989; *Barker* and *Nixon*, 1989; *Le Bas*, 1989; *Nygwena* and *Bailey*, 1990) have firmly established the existence of carbonatite magmas with high Ca content. It has been suggested that sövite is formed by crystal fractionation of dolomitic carbonatite (*Gittins* 1988, 1989), or by loss of a vapor phase rich in alkalies from natrocarbonatite (*Le Bas*, 1987). We consider that the Shombole carbonatite dikes, tuffs, and im-

miscible globules demonstrate that sövite magma can be primary, in the sense that it need not be generated by crystal or vapor fractionation of carbonatite magma with radically different composition.

The highly sodic lavas of Oldoinyo Lengai contrast strongly with the Shombole nephelinites (which are typical of most alkali silicate/carbonatite complexes). Some nephelinites from Oldoinyo Lengai are extremely peralkaline ([Na + K]/Al $\approx$ 2) and rich in phenocrysts of sodalite and combeite ($Na_2Ca_2Si_3O_9$) (*Peterson* and *Marsh*, 1986; *Peterson*, 1989; *Dawson* et al., 1989; *Keller* and *Krafft*, 1990). In comparison, Shombole nephelinites are only moderately peralkaline ([Na + K]/Al = 1.1–1.2). The Lengai combeite nephelinites are virtually identical in composition to the silicate liquids shown by *Freestone* and *Hamilton* (1980) to be immiscible with natrocarbonatite, and contain carbonate/zeolite globules similar to those described above.

The experimental production of silicate-carbonate liquid immiscibility in lavas from Shombole and Oldoinyo Lengai, together with the congruence between natural and experimental mineral and liquid compositions, supports the hypothesis that the sövites of Shombole and the natrocarbonatites of Oldoinyo Lengai originated by liquid immiscibility. This congruence is evident in Fig. 9, where whole rock nephelinite compositions from both centers are plotted in SCAN and compared to the silicate limbs of the experimentally determined two-liquid fields. The relationship between peralkalinity and the two-liquid solvus is well displayed by these data. The Shombole nephelinites define a trend which is virtually identical to the silicate limb of the solvus, consistent with the hypothesis that fractionation of an immiscible carbonate liquid in conjunction with solid phases controls the compositional trends displayed by these rocks (*Kjarsgaard* and *Hamilton* 1989b).

Since there is no evidence for Mg- or (Na + K)-rich carbonatites at Shombole or (Mg, Ca)-rich carbonatites at Oldoinyo Lengai, hypotheses involving crystal frac-

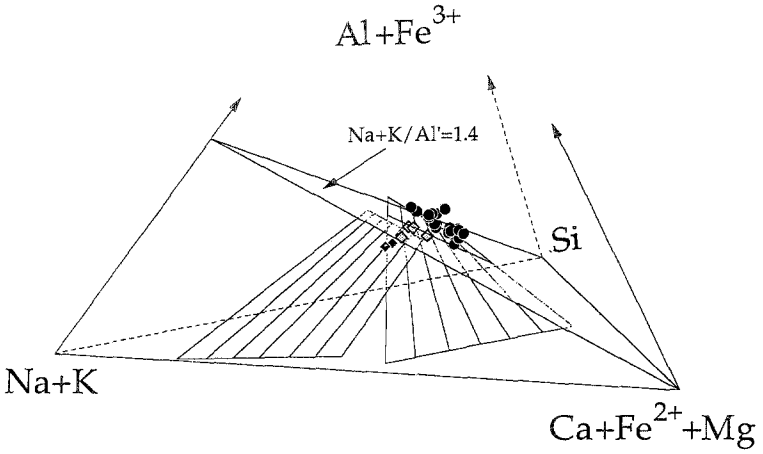

Fig. 9. Projections of whole rock nephelinite compositions from Shombole (filled circles) and Oldoinyo Lengai (diamonds) onto SCAN (data from *Peterson* 1989a). The diamonds and silicate limb of the experimentally determined 300 MPa Lengai solvus all lie below the plane (Na + K)/Al′ = 1.4; filled circles and the silicate limb of the experimentally determined Shombole 500 MPa polythermal solvus all lie above the plane (Na + K)/Al′ = 1.4. Data are plotted in atomic %

tionation to produce one carbonatite from another seem unnecessary. A viable model would be that both sövite and natrocarbonatite magma are generated by liquid immiscibility from evolved carbonated nephelinite, but that the formation of natrocarbonatite requires the presence of unusually peralkaline bulk compositions. *Peterson* (1989b) suggested that Lengai-type nephelinites are the fractionation products of olivine-melilite nephelinites, whereas less alkaline (Shombole-type) nephelinites are produced by crystal fractionation of olivine nephelinite, a relatively common magma type in the East African Rift.

This model can be extended to Mg-rich carbonatites if it is assumed that olivine nephelinites, which are more primitive than Shombole and Lengai-type nephelinites (containing $\leq 3\%$ MgO), can also become saturated with a CO_2-rich liquid phase at lower crustal pressures. The appropriate studies have not been made, but we predict that carbonatitic liquids rich enough in Mg to crystallize olivine and dolomite upon cooling, will be found in future experimental research utilizing primitive carbonated olivine nephelinites. Although this would remove the restriction for Mg-rich carbonatites to be directly derived from the mantle (*Gittins* 1988, 1989), it is possible that magnesian (and most other!) carbonatites have more than one origin.

Logically, ferrocarbonatites might be exsolved from very Fe-rich nephelinitic or phonolitic liquids, but we are not aware that any corresponding silicate lavas have been found, and a nonprimary origin for ferrocarbonatite seems likely. The authors disagree on the origin of ferrocarbonatites. One of us (BAK) supports an origin by crystal accumulation of siderite, magnetite, etc. from dolomitic or sövitic magmas at low oxygen fugacities, and the other (TDP) prefers to invoke reaction of sövite (or rauhaugite, etc.) magma with cumulates rich in magnetite, Fe-rich clinopyroxene, etc. derived from cogenetic silicate rocks. There is much need for further detailed field and experimental studies of these fascinating and complex rocks.

Summary

Nephelinites from Shombole volcano, East Africa, contain globules rich in calcite plus other phases with high Ba, Sr, P, and F. They are interpreted as immiscible carbonatite globules on the basis of their mineralogical composition (typical for a carbonatite) and their textures, which are most consistent with an origin by crystallization of carbonatite liquid drops. The thermodynamic conditions for equilibrium liquid immiscibility are well satisfied, since the mineral assemblages and compositions within the droplets closely match those in the silicate groundmass, which is interpreted as the crystallized conjugate liquid. The existence of a two-liquid field is confirmed experimentally, and the original assemblages in the lavas (2 liquids + crystals) are exactly duplicated in the experiments. The experiments indicate that the two-liquid field was intersected by most Shombole nephelinites near 960 °C, in good agreement with calculated eruption temperatures for the lavas (840–950 °C).

The carbonatite globules, dikes, and tuffs at Shombole are all Ca-rich and are classified as sövite. In contrast, both natural carbonatite lavas at Oldoinyo Lengai, and immiscible carbonate liquids generated experimentally using Lengai-type bulk compositions, are rich in Na + K and are classified as natrocarbonatite. The field, petrographic, and experimental data do not support the hypothesis that sövite and natrocarbonatite are related by crystal and/or vapor fractionation. We interpret

both types of carbonatite to originate by liquid immiscibility from carbonated nephelinites or phonolites with strongly contrasting peralkalinity. We speculate that Mg-rich carbonatites may be exsolved from primitive carbonated olivine nephelinites, and that the spectrum of carbonatite compositions is reflected in the known range of nephelinite compositions. The exception is ferrocarbonatite, which has no silicate analogue and is probably formed by secondary processes such as crystal fractionation/accumulation, or crystal/liquid reaction.

Acknowledgements

Financial assistance from the NERC (grant GR3/6477) to *D. L. Hamilton* for the experimental petrology lab, and financial assistance from the University of Manchester and the CVCP to BAK are gratefully acknowledged. *M. Bonardi* (Ottawa) and *D. Plant* (Manchester) provided highly capable assistance with the microprobe analyses. Reviews by *R. Macdonald* and two anonymous referees greatly improved the manuscript. This is GSC contribution #15390.

References

Baker BH (1963) Geology of the area south of Magadi. Geol Surv Kenya Report #42

Barker DS (1989) Field relations of carbonatites. In: *Bell K* (ed) Carbonatites: genesis and evolution. Unwin Hyman, London, pp 38–69

— *Nixon PH* (1989) High-Ca, low-alkali carbonatite volcanism at Fort Portal, Uganda. Contrib Mineral Petrol 103: 166–177

Bell K, Peterson TD (in press) Nd and Sr isotope systematics of Shombole volcano, East Africa, and the links between nephelinites, phonolites, and carbonatites. Geology

Bowen NL (1928) The evolution of the Igneous Rocks. Dover Publications, Toronto

Crossley R (1979) The Cenozoic stratigraphy and structure of the western part of the rift valley in southern Kenya. J Geol Soc London 136: 393–405

Dawson JB (1962) The geology of Oldoinyo L'engai. Bulletin Volcanologique 24: 349–387

— (1989) Sodium carbonate extrusions from Oldoinyo Lengai, Tanzania: implications for carbonatite complex genesis. In: *Bell K* (ed) Carbonatites: genesis and evolution. Unwin Hyman, London, pp 255–277

— *Smith JV, Steele IM* (1989) Combeite $(Na_{2.33}Ca_{1.74}others_{0.12})Si_3O_9$ from Oldoinyo L'engai, Tanzania. J Geol 97: 365–372

Deans T, Roberts R (1984) Carbonatite tuffs and lava clasts of the Tinderet foothills, western Kenya: a study in calcified natrocarbonatites. J Geol Soc London 141: 563–580

Eggler DH (1978) The effect of CO upon partial melting of peridotite in the system Na_2O–CaO–Al_2O_3–MgO–SiO_2–CO_2 to 35 kb, with an analysis of melting in a peridotite–H_2O–CO_2 system. Am J Sci 278: 305–343

— (1989) Carbonatites, primary melts, and mantle dynamics. In: *Bell K* (ed) Carbonatites: genesis and evolution. Unwin Hyman, London, pp 561–579

Fairhead JD, Mitchell JD, Williams LJ (1972) New K/Ar determinations on rift volcanics of S. Kenya and their bearing on age of rift faulting. Nature 238: 66–69.

Freestone IC, Hamilton DL (1980) The role of liquid immiscibility in the genesis of carbonatites: an experimental study. Contrib Mineral Petrol 73: 105–117

Gittins J (1988) The origin of carbonatites. Nature 335: 295–296

— (1989) The origin and evolution of carbonatite magmas. In: *Bell K* (ed) Carbonatites: genesis and evolution. Unwin Hyman, London, pp 580–600

Hamilton DL, Freestone IC, Dawson JB, Donaldson CH (1979) Origin of carbonatites by liquid immiscibility. Nature 279: 52–54

— *Bedson P, Esson J* (1989) The behaviour of trace elements in the evolution of carbonatites. In: *Bell K* (ed) Carbonatites: genesis and evolution. Unwin Hyman, London, pp 405–427

Hay RL (1983) Natrocarbonatite tephra of Kerimasi volcano, Tanzania. Geology 11: 599–602

Helz GR, Wyllie PJ (1979) Liquidus relationships in the system $CaCO_3$–$Ca(OH)_2$–CaS and the solubility of sulphur in carbonatite magmas. Geochim Cosmochim Acta 43: 259–265

Javoy M, Pineau F, Cheminee JL, Kraft M (1988) The gas-magma relationship in the 1988 eruption of Oldoinyo Lengai (Tanzania). EOS 69: 1466

Keller J (1981) Carbonatitic volcanism in the Kaiserstuhl alkaline complex: evidence for highly fluid carbonatitic melts at the Earth's surface. J Volcanol Geothermal Res 9: 423–431

— (1989) Extrusive carbonatites and their significance. In: *Bell K* (ed) Carbonatites: genesis and evolution. Unwin Hyman, London, pp 70–88

— *Krafft M* (1990) Effusive natrocarbonatite activity of Oldoinyo Lengai, June 1988. Bull Volcan 52(8): 629–645

King BC, Sutherland DS (1966) The carbonatite complexes of eastern Uganda. In: *Tuttle OF, Gittins J* (eds) Carbonatites. John Wiley and Sons, London, pp 73–126

Kim KT, Burley BJ (1971) Phase equilibria in the system $NaAlSi_3O_8$–$NaAlSiO_4$–H_2O Up to 15 Kb. A theoretical discussion. Can J Earth Sci 8(5): 549–557

Kjarsgaard BA (1990) Nephelinite-carbonatite genesis: experiments on liquid immiscibility in alkali silicate-carbonate systems. Unpublished Ph.D. thesis, University of Manchester, England

— *Hamilton DL* (1988) Liquid immiscibility and the origin of alkali-poor carbonatites. Mineral Mag 52: 43–55

— *Hamilton DL* (1989a) Carbonatite origin and diversity. Nature 338: 547–548

— (1989b) Melting experiments on Shombole nephelinites: silicate/carbonate liquid immiscibility, phase relations and the liquid line of descent. Geolog Assoc Canada/ Min Assoc Canada Program with Abstracts 14, A50

— (1989c) The genesis of carbonatites by immiscibility. In: *Bell K* (ed) Carbonatites: genesis and evolution. Unwin Hyman, London, pp 388–404

Koster van Groos AF, Wyllie PJ (1966) Liquid immiscibility in the system Na_2O–Al_2O_3–SiO_2–CO_2 at pressures up to 1 kilobar. Am J Sci 264: 234–255

— (1968) Liquid immiscibility in the join $NaAlSi_3O_8$–Na2CO_3–H_2O. Am J Sci 266: 932–967

— (1973) Liquid immiscibility in the join $NaAlSi_3O_8$–$CaAl_2Si_2O_8$–Na_2CO_3–H_2O. Am J Sci 273: 465–487

Le Bas MJ (1987) Nephelinites and carbonatites. In: *Fitton JG, Upton BGJ* (eds) Alkaline igneous rocks. Blackwell, London, pp 53–85

— (1989) Diversification of carbonatite. In: *Bell K* (ed) Carbonatites: genesis and evolution. Unwin Hyman, London, pp 428–447

Levin EM, Robbins CR, McMurdie HF (1964) Phase diagrams for ceramists. The American Ceramic Society, Inc. Columbus, Ohio.

Ngwenya BT, Bailey DK (1990) Kaluwe carbonatite, Zambia: an alternative to natrocarbonatite. J Geol Soc London 147: 213–216

Peterson TD (1989a) Peralkaline nephelinites I. Comparative petrology of Shombole and Oldoinyo L'engai, East Africa. Contrib Mineral Petrol 101: 458–478

— (1989b) Peralkaline nephelinites II. Low pressure fractionation and the hypersodic lavas of Oldoinyo L'engai. Contrib Mineral Petrol 102: 336–346

— (1990) Petrology and genesis of natrocarbonatite. Contrib Mineral Petrol 105: 143–155

— *Marsh BD* (1986) Sodium metasomatism and mineral stabilities in alkaline ultramafic rocks: implications for the origin of the sodic lavas of Oldoinyo L'engai. EOS 67: 389–390

Roedder E (1979) Silicate liquid immiscibility in magmas. In: *Yoder HS* (ed) The evolution of the igneous rocks. Princeton University Press, Princeton, pp 15–58

Sack RO, Carmichael ISE, Rivers M, Ghiorso MS (1981) Ferric-ferrous equilibria in natural silicate liquids at 1 bar. Contrib Mineral Petrol 75: 369–376

Twyman JD, Gittins J (1987) Alkalic carbonatite magmas: parental or derivative? In: *Fitton JG, Upton BGJ* (eds) Alkaline igneous rocks. Blackwell, London, pp 85–94

Verwoerd WJ (1978) Liquid immiscibility and the carbonatite-ijolite relationship: preliminary data on the join $NaFe^{3+}Si_2O_6$–$CaCO_3$ and related compositions. Carn Inst Wash Ybk 77: 767–774

Wallace ME, Green DH (1988) An experimental determination of primary carbonatite magma composition. Nature 335: 343–346

Wendlandt RF, Harrison WJ (1979) Rare earth partitioning between immiscible carbonate and silicate liquids and CO_2 vapor: results and implications for the formation of light rare earth-enriched rocks. Contrib Mineral Petrol 69: 409–419

Wyllie PJ (1978) Mantle fluid compositions buffered in peridotite-CO_2–H_2O by carbonates, amphibole, and phlogopite. J Geol 86: 687–713

— (1989) Origin of carbonatites: evidence from phase equilibrium studies. In: *Bell K* (ed) Carbonatites: genesis and evolution. Unwin Hyman, London, pp 500–545

Authors' address: Dr. *B. Kjarsgaard* and Dr. *T. Peterson*, Geological Survey of Canada, 601 Booth Street, Ottawa, Canada K1A OE8.